DISTRIBUTED TARGET LOCALIZATION AND TRACKING WITH WIRELESS PYROELECTRIC SENSOR NETWORKS

Baihua Shen [1,2], Guoli Wang [1]

[1] School of Information Science & Technology, Sun Yat-Sen University,

Guangzhou, Guangdong, 510006, China

[2] School of Information Engineering, Guangdong University of Technology,

Guangzhou, 510006, China

Email: bhshen@sohu.com

Submitted: Feb.21, 2013 ***Accepted: July 16, 2013*** ***Published: Sep.3, 2013***

Abstract- Due to the disadvantages of traditional localization & tracking at those aspects of users' privacy protection, system configuration and maintenance, this paper proposes a new approach for infrared object localization and tracking with distributed wireless pyroelectric infrared sensors. A hierarchical architecture of visibility of Fresnel lens array is presented with spatial-modulated field of view (FOV). Firstly, the FOVs of Fresnel lens array in a sensor node are modulated to achieve a single degree of freedom (DOF) spatial partition; then the localization algorithm is proposed to coordinate multiple sensors nodes to achieve two DOF spatial partitions. To effectively solve the problem of WSN energy imbalance, a strategy of neighbor table multicast and an electoral method of the dynamic cluster head based on the biggest energy are presented in the distributed wireless sensor networks. The experiments show that the method proposed here has the advantages in high accuracy and strong anti-interference capability.

Index terms: Wireless sensor networks, motion detecting, target localization, target tracking, pyroelectric infrared.

I. INTRODUCTION

Target localization and tracking, the common key technology and the controversial research hotspot in intelligent monitoring, advanced human-machine interaction [1] , motion analysis [2-6], activity understanding [7-9], are of widely application value in calamities aiding, security monitoring, medical monitoring, etc. PIR detector, in a form of non-contact, detects infrared radiation variation in the specific environment with high sensitivity to human motion and the advantages of low cost, non-invasion, strong concealment and little interference by ambient light. The localization and tracking by PIR detector have been receiving increased attention.

Two major types of PIR sensing methods are adopted in pre-existing research, that is side view [10-15] and top view [16, 17].

In side view sensing research, paper [10] proposes passive infrared sensing model based on wireless sensor networks (WSN), which combines many sensors to form horizontal regional subdivisions of FOV, hence, achieves the human motion localization and tracking. Researched in paper [11], to obtain the object's position, the PIWSNTT system synthesizes many object azimuth data sensed by passive infrared sensor nodes. But this method, relying on restricted condition of object keeping uniform linear movement, cannot manage the situation of constant turn-back movement. In paper[12-14], the horizontal angle modulation method is adopted to obtain object's local fine granularity localization, tracking and identification, but these side-view sensing methods above are not applicable when the object is shielded by obstacles, therefore, their applicability are quite limited.

In top view sensing research, PILAS system, proposed in paper [17], cross many PIR detectors' top view FOV for regional division to realize object motion detecting and coarse granularity localization. Compared with side view sensing, it can effectively overcome the problem of obstacles shielding. Since the sensed granularity is depended on the scale of FOV

crossed area, in order to obtain fine granularity sensibility, the numbers of sensors should be increased by leaps and bounds. For example, if the location accuracy is 0.5m, one sensor node should be placed every 1m distance. That is far from the efficiency of side view sensing, therefore, sensibility improving is restricted by coarse granularity sensing.

In order to solve the above-mentioned problems, in this paper, FOV modulation strategy is introduced into top view sensing mode to make it possess fine granularity sensibility. For different sensing view angle, the horizontal angle modulation method in side view sensing mode in paper [12] is not suitable for top view sensing mode. Therefore, this paper proposes radial distance modulation method. Particularly, this paper applies hierarchical structure and multiplexing system to spatially modulate the FOV of Fresnel lens array, to establish FOV modulation mode and localization model in spatial juxtaposition and to attribute movement spatial localization to multivariant FOV subdivision, which is formed by many collaboration sensors of single degree of freedom (SDOF) FOV subdivision for object localization. The method, extracting information directly from the radiation source's movement characteristics and spatial position, applies to large-scale WSN space deployment, because of low cost data transport and processing.

In large-scale WSN, due to limited resources and energy of a single node, the centralized telecommunication and information processing lead to energy consumption of each node unbalanced and especially center node possibly paralyzed and then the whole network. Therefore, distributed localization and tracking method can effectively solve the problem of WSN energy imbalance. According to the characteristics of infrared object localization and tracking, this paper implements the multicast strategy within moving nodes by establishing a neighbor table with six neighborhoods and presents an electoral method of the dynamic cluster head based on the biggest energy and distributed calculation algorithm.

II. HIERARCHIAL STRUCTRURE MODEL

a. Pyroelectric Sensor Model

Define $s(r,t)$ as the infrared radiation field function of radiation source, where r represents position, and t represents time, state space (object space) as the two dimensions plane space where infrared radiation source moving and measurement space as the point set of the location of each sensor node. Reference structure modulates the visibility from source space to measurement space.

Define $v(r_i,r)$ or $v_i(r)$ as the visibility function between point r in source space and point r_i in measurement space. $v(r_i,r)\in[0,1]$, the bigger the value of $v(r_i,r)$, the better the visibility, in which, "1" stands for fully visible, while "0" completely invisible.

The response signal of a PIR detector at point r_i is given by

$$m(r_i,t)=\int h(t-t')v(r_i,r)s(r,t)d\ r \quad i\in\{1,2,\cdots,M\} \tag{1}$$

Where $h(t)$ is the impulse response of PIR detector. Sensing model is showed in Figure 1.

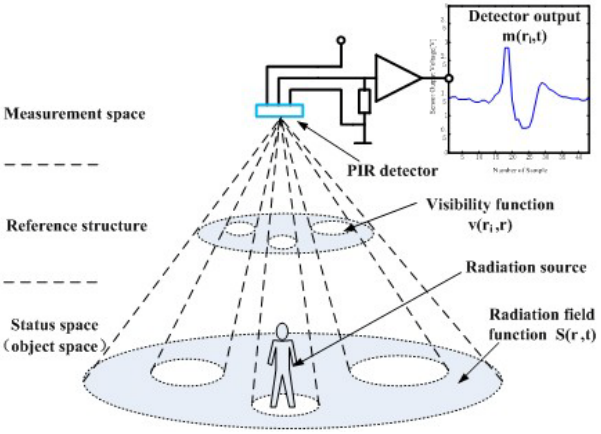

Figure 1. Sensing model of PIR detector

b. Discrete Model

Define C as the state space. We divide C into L cells, defined as $C_j\left(j\in\{1,2,\cdots,L\}\right)$.

$$\bigcup_{i=1}^{L}C_i=C \tag{2}$$

$$C_i\cap C_j=\varnothing \quad (i,j\in\{1,2,...L\} \text{ and } i\neq j\ ) \tag{3}$$

Thus formula (1) can be described as the discrete non-isomorphic model

$$\mathbf{m} = \mathbf{Vs} \tag{4}$$

Where $\mathbf{m}$ is a M dimensional vector of measurement space, $\mathbf{m} = [m_i](i = 1, 2, \cdots, M)$; $\mathbf{V}$ represents visibility matrix, decided by the modulated strategy of radiation field, $\mathbf{V} = [v_{ij}](i = 1, 2, \cdots, M; j = 1, 2, \cdots, L)$; and $\mathbf{s}$ is the state vector, its dimension is decided by the cells number of state space, $\mathbf{s} = [s_j](j = 1, 2, \cdots, L)$.

c. Boolean sensing model

In Boolean sensing model, m_i, v_{ij} and s_j are binary value. v_{ij}=1, if and only if C_j is visible to ith (number i) PIR detector, otherwise, v_{ij}=0; s_j=1, if and only if the position of the object (radiation source) is in C_j, otherwise, s_j=0. The output of ith detector

$$m_i = \vee v_{ij} s_j \tag{5}$$

Where "$\vee$" represents Boolean sum. This is called Boolean sensing model in this paper, whose output is a binary value.

Boolean sensing model improves the reliability of infrared sensing, and decreases the data size of data gathering and transmission process. The light-weight non-isomorphic sensing model turns complicated sampling of object space into simple binary state sampling process, and what need to be obtained is only to know in which sampling cell the object appears. This direct measurement of motion states can meet the needs of most target localization and tracking task.

The output of M detectors in measurement space is a M dimensional vector, and there are 2^M different values. Excluding zero vector, it can divide state space into $2^M - 1$ cells at most, that is $L \le 2^M - 1$. Define η as the sensing efficiency,

$$\eta = \frac{\log_2(L+1)}{M} \tag{6}$$

$\eta \in [0,1]$, given the value of M, the bigger of the value of L, the higher the sensing efficiency. When $L = 2^M - 1$, $\eta = 100\%$.

III. MODULATION STRATEGY BASED ON RADIAL DISTANCE

A single PIR detector can only output two different states and cannot be used to measure distances between the radiation object and detector. In order to estimate the position of an infrared radiation object, the problem of the location of object state space is down to multi-degree of freedom FOV division in this paper. At first a radial distance modulated method is proposed, therefore the distance between object and detector can be measured by several PIR detectors in a single sensor node, and then with several sensor nodes data fusion，the position of the object can be estimated.

The Fresnel lens array equipped on PIR detector cannot only enhance perception sensitivity, but also modulate its infrared visibility by infrared absorption or mask material. By designing the visibility of Fresnel lens array properly, we not only acquire motion characteristic information directly and effectively, but also simplify the data processing greatly.

The FOV of a PIR detector with hemispherical Fresnel lens array is a cone-shape space, and its projection on the ground plane is an area with several concentric rings. The FOV of a PIR detector with 7-ring hemispherical Fresnel lens array is showed in Figure 2.

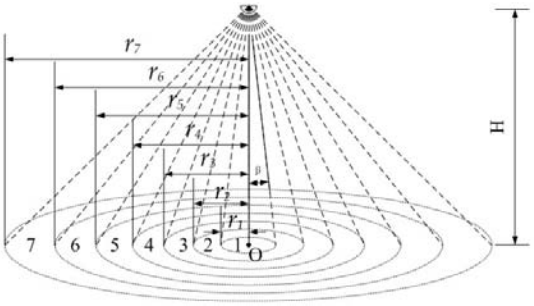

Figure 2. FOV of a PIR detector with hemispherical Fresnel lens array

Due to the restrictions of physical characteristics of the Fresnel lens array, a n-ring hemispherical lens array divides its FOV into n concentric rings, therefore, we can achieve this functionality by using M ($M \geq [\log_2(n+1)]$) PIR detectors.

As an example, if $n=7$, $M \geq \log_2(7+1)=3$. The sensing model reaches its maximum efficiency when $M=3$.

Gray code was applied in our model to encode the output of M detectors, which is a minimize-error code where two successive values differ in only one bit, thus gray code reduces the impact of error code on measuring result. An example of 3-bit wide gray code is listed in Table 1.

Table 1: 3-bit wide gray code

No.	Bit 1	Bit 2	Bit 3	No.	Bit 1	Bit 2	Bit 3
1	0	0	1	5	1	1	1
2	0	1	1	6	1	0	1
3	0	1	0	7	1	0	0
4	1	1	0	8	0	0	0

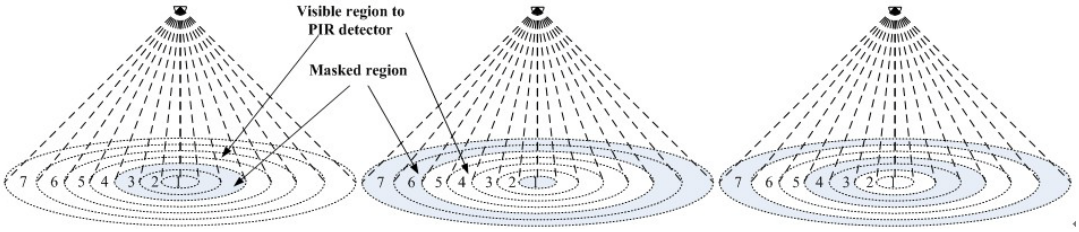

Figure 3. Modulation strategy based on radial distance

Table 2: Output parameters of each detector

Rings No.	Detectors outputs			Range of horizontal distance to detector center	Estimated horizontal distance	Which detectors can sense object
	s1	s2	s3			
1	0	0	1	$0 \sim r_1$	$r_1 / 2$	s3
2	0	1	1	$r_1 \sim r_2$	$(r_1 + r_2) / 2$	s2 s3
3	0	1	0	$r_2 \sim r_3$	$(r_2 + r_3) / 2$	s2
4	1	1	0	$r_3 \sim r_4$	$(r_3 + r_4) / 2$	s1 s2
5	1	1	1	$r_4 \sim r_5$	$(r_4 + r_5) / 2$	s1 s2 s3
6	1	0	1	$r_5 \sim r_6$	$(r_5 + r_6) / 2$	s1 s3
7	1	0	0	$r_6 \sim r_7$	$(r_6 + r_7) / 2$	s1

According to the order of gray code as showed in Table 1, we use masks to restrict the FOV of each Fresnel lens array. The restriction region of each Fresnel lens array is the shading pattern as showed in Figure 3. The object can't be detected by the PIR detector if it is in the

shading areas. The outputs of 3 detectors are listed in Table 2 when the object is located in each different ring area, thus on the basis of the modulation strategy, the horizontal distance between the object and the detectors can be estimated.

IV. ALGORITHM OF COOPERATIVE LOCALIZATION

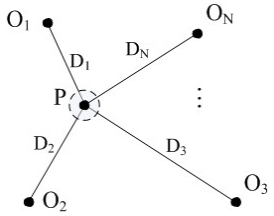

Figure 4. Cooperative localization with multiple sensor nodes

According to the theory of trilateration, when the distance between the object and each sensor node has been estimated, the position of the object can be estimated too. Define $O_i(\overline{x}_i, \overline{y}_i)$ (i= *1,2,...,N* as the position of the sensor node center in Cartesian coordinate and $P(x, y)$ as the position of the object, which are showed in Figure 4. The measured distance of each sensor node is D_i, thus we have the over-determinant equations,

$$(x-\overline{x}_i)^2+(y-\overline{y}_i)^2=D_i^2, \qquad (i=1,2,...,N) \tag{7}$$

Matrix form of the over-determinant equations is

$$\mathbf{Hx}=\mathbf{f} \tag{8}$$

Where

$$\mathbf{H}=2\begin{pmatrix} \overline{x}_2-\overline{x}_1 & \overline{y}_2-\overline{y}_1 \\ \overline{x}_3-\overline{x}_2 & \overline{y}_3-\overline{y}_2 \\ \overline{x}_3-\overline{x}_1 & \overline{y}_3-\overline{y}_1 \end{pmatrix}, \quad \mathbf{x}=\begin{pmatrix} x \\ y \end{pmatrix}, \quad \mathbf{f}=\begin{pmatrix} D_1^2-D_2^2+\overline{x}_2^2-\overline{x}_1^2+\overline{y}_2^2-\overline{y}_1^2 \\ D_2^2-D_3^2+\overline{x}_3^2-\overline{x}_2^2+\overline{y}_3^2-\overline{y}_2^2 \\ D_1^2-D_3^2+\overline{x}_3^2-\overline{x}_1^2+\overline{y}_3^2-\overline{y}_1^2 \end{pmatrix}$$

The least squares solution of $\mathbf{x}$ is

$$\mathbf{x}=\left(\mathbf{H}^{\mathrm{T}}\mathbf{H}\right)^{-1}\mathbf{H}^{\mathrm{T}}\mathbf{f} \tag{9}$$

V. DISTRIBUTED LOCALIZATION ALGORITHM

Deployment diagram of large-scale WSN is showed in Figure 5. Define d as the distance between two adjacent nodes. The projection on the ground plane of FOV of the sensor node $a_{i,j}$ is a circle area centered at the node center, whose radius is d. Define a WSN node as the active node, when the object appears in the scope of its FOV. Except a few routing nodes, all other inactive nodes can turn into sleep mode to save energy. When infrared object moves into the perception scope of sensor node, the sensor node will be awaked by the high level signal issued by PIR detectors.

The object at any place of the whole WSN area, except some edge region, can be sensed by at least three WSN nodes, and three of these active nodes, adjacent to each other, were selected as task nodes to estimate the position of the object. For instance, when the object is at the red triangle point, as showed in Figure 5, node $a_{i-1,j-1}$, $a_{i-1,j}$ and $a_{i,j}$ are active nodes, meanwhile, they are also task nodes.

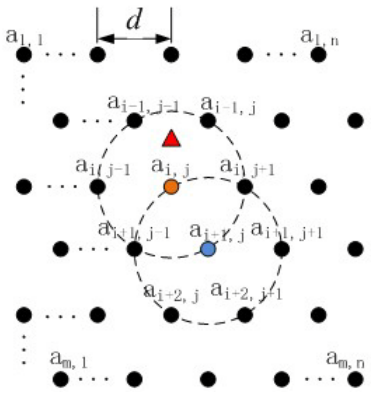

Figure 5. Deployment diagram of WSN

a. Neighbor table and multicast strategy

As mentioned before, three task nodes compose a basic localization module, and these task nodes only need to transfer its output to its neighbor node. To establish neighbor table and apply multicast telecommunication way in the tables can greatly reduce the communication data between each sensor node, save node energy consumption and prolong the network life cycle. Define $N(a_{i,j})$ as the neighbor node of node $a_{i,j}$:

(1) If i is an odd number

$N(a_{i,j}) \in \{a_{k,l} \mid |k-i| \le 1, 0 \le j-l \le 1\}$

or $N(a_{i,j}) \in \{a_{k,l} \mid k = i, l = j+1\}$

As an example, in Figure 5, all nodes in circle centered at the node $a_{i,j}$, whose radius is d, are the neighbor node of $a_{i,j}$, that is $N(a_{i,j}) \in \{a_{i-1,j-1}, a_{i-1,j}, a_{i,j-1}, a_{i,j+1}, a_{i+1,j-1}, a_{i+1,j}\}$.

(2) If i is an even number

$N(a_{ij}) \in \{a_{k,l} \mid |k-i| \le 1, 0 \le l-j \le 1\}$

or $N(a_{ij}) \in \{a_{k,l} \mid k = i, l = j-1\}$

As an example, in Figure 5, $N(a_{i+1,j}) \in \{a_{i,j}, a_{i,j+1}, a_{i+1,j-1}, a_{i+1,j+1}, a_{i+2,j}, a_{i+2,j+1}\}$.

Define $G(a_{i,j}) = (i-1)*n + j$ as the serial number of node $a_{i,j}$. Node $a_{i,j}$ and its all neighbor nodes are added to a group. Choose $G(a_{i,j})$ as the group serial number, and one node might be granted to multiple groups. When active node $a_{i,j}$ has sensed the motion of object, it sends a multicast packet to all its neighbor nodes with the group serial number $G(a_{i,j})$. This multicast strategy assures inactive node couldn't receive the multicast packet, which decreases energy loss of WSN node, and prolong the WSN lifecycle.

b. Algorithm of Cluster Head Election

Three task nodes which are adjacent each other can be regarded as member nodes of a cluster, and we need to elect a cluster head from these task nodes to estimate the position of the object based on least-square algorithm, and to send position data to PC for store and display. Since the object is always in the course of movement and task nodes change accordingly, that is, member nodes of the cluster change accordingly. For the balance of energy consumption of each node, a cluster-head election algorithm based on maximum residual energy is applied in this paper, that is, the task node that has the maximum residual energy will be elected as the cluster head. The algorithm of cluster head election and distributed localization is listed as follows:

1) Initialization: set coordinate of each sensor node, build neighbor table, and set group serial number;

2) Sensor nodes switch to sleep mode by shutting down system clock to reduce energy consumption, without any motion detecting information of the object during a certain time;

3) Node $a_{i,j}$ will be waked up to normal mode by the high-level outputs of PIR detectors immediately as soon as the object moves to its sensing region;

4) Node $a_{i,j}$ check whether received packets from other two task nodes, if yes, then to next step, otherwise, go to step 7;

5) Node $a_{i,j}$ extracts the residual energy messages of the other two task nodes, and check whether its own residual energy is the maximum, if yes, elect itself as cluster head, otherwise, go to step 7;

6) Estimate the position of the object based on least-square or look-up table algorithm as mentioned before, and send calculation result packet to PC (through router or coordinator), then go to step 2;

7) Node $a_{i,j}$ sends a multicast packet, which includes its residual energy, position coordinate and measurement result of its horizontal distance to the object, to its all neighbors with the group serial number $G(a_{i,j})$, then go to step 2.

VI. EXPERIMENTS

a. Hardware configuration of WSN node

A WSN node consists of three modules: CPU and radio communication module, PIR detectors module and power module. Chip CC2530 is used in CPU and radio communication module, which is the second generation system-on-chip solution for 2.4 GHz IEEE 802.15.4. PIR detectors module include three PIR detectors and three Fresnel lens arrays. Photos of sensor node are listed in Figure 6 and Figure 7.

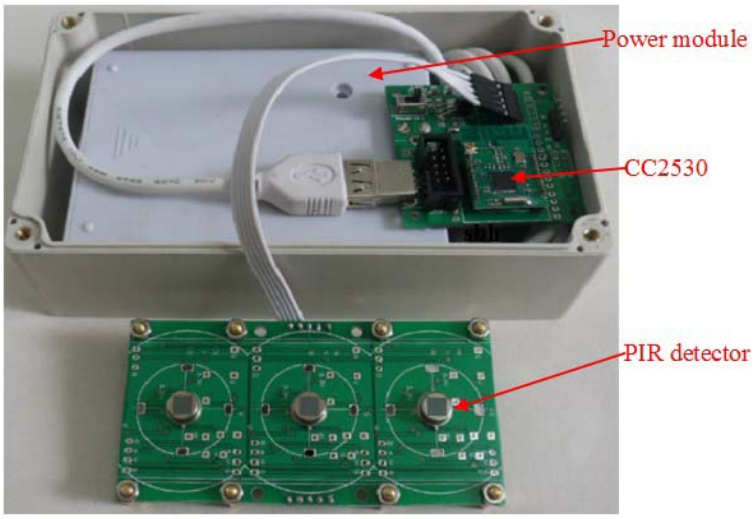

Figure 6. Hardware prototype

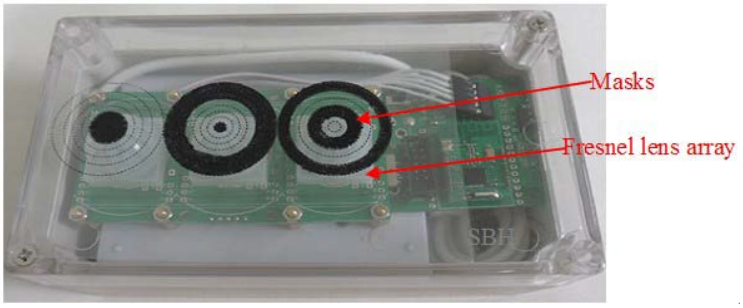

Figure 7. Assembled WSN node

b. Experimental environment and parameters

The network including 11 WSN nodes is deployed under the ceiling, 300cm height from ground, in an indoor environment with the size of 900cm*520cm. Relative parameters in Figure 2 and Figure 5 are listed in Table 3, and the maximum theoretical error of radial distance is $(r_7 - r_6)/2 = 31.5$ cm.

Table 3: Experimental parameters

Parameter	Value	Unit	Parameter	Value	Unit
H	300	cm	r_3	106	cm
d	300	cm	r_4	145	cm
β	6.5	degree	r_5	191	cm
r_1	34	cm	r_6	242	cm
r_2	69	cm	r_7	305	cm

Figure 8 is the layout of WSN nodes. The black circles represent the locations of sensor nodes, the number in the black circle represent the serial number $G(a_{i,j})$ of node $a_{i,j}$. In Figure 9 the red ellipses represent the locations of sensor nodes in the real environment.

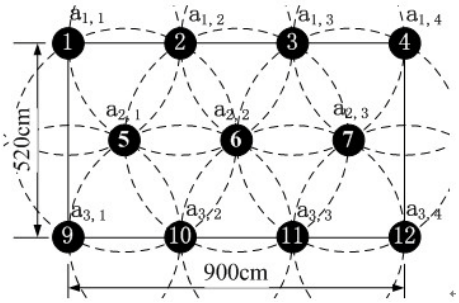

Figure 8. Layout of WSN nodes

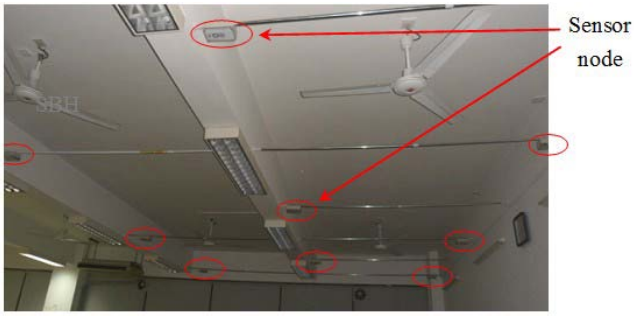

Figure 9. Deployment photo of WSN nodes that correspond to Figure 8

c. Tracking experiment of a smart toy car

An autonomous tracing smart toy car, at uniform speed v and act as the tracked object by WSN, is used in this experiment, and a bottle of hot water with temperature at 37 degrees Celsius, mounted on the smart car, is chosen as the infrared radiation source.

(1)"8"-shape path tracking

Motion path of the smart car is showed in Figure 10, and its velocity $v = 100cm/s$.

In Figure 11 red solid line represents the actual motion path, red solid line with circle represents the original localization result of WSN nodes with least-square algorithm, and black solid line with asterisk represents the tracking result of block Extended Kalman Filter (EKF) algorithm, and blue solid line with box represents the localization result of mean filter algorithm. It can be seen that mean filter algorithm is better than EKF algorithm in this curve tracking experiment. Figure 12 shows the histogram of localization errors of the mean filter algorithm. It can be seen that the distribution of the localization errors follow a normal distribution closely. Table 4 shows the parameters of localization errors of direction X and

direction Y. The maximum localization error in X and Y direction is 38 cm, and 68 percent of absolute value of these localization errors are less than 18 cm.

Table 4: Localization errors with “8”-shape path

Localization error of direction X (cm)			**Localization error of direction Y (cm)**		
Mean	Standard deviation	Maximum	Mean	Standard deviation	Maximum
12.2	9.3	37.5	11.6	9.0	38.3

Figure 10. “8”-shape route

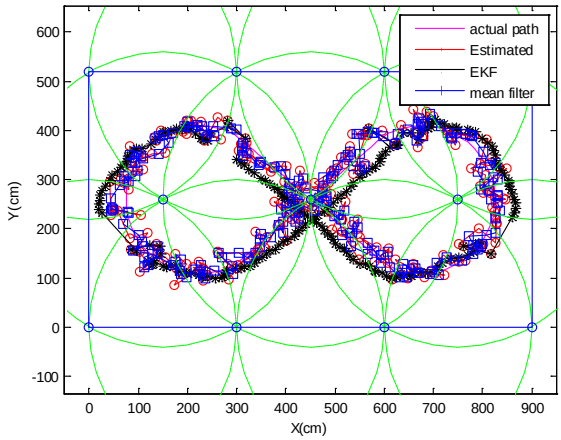

Figure 11. “8”-shape route tracking

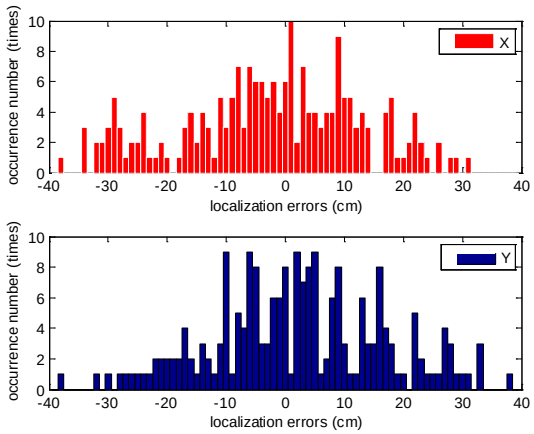

Figure 12. Histogram of localization error

（2）rectangular path tracking

In this tracking experiment, we change the tracking path to a rectangular path with length 600 cm and width 300 cm. The legend meaning in Figure 13 is the same as Figure 11. It can be seen from Figure 14, the maximum localization errors in direction X and Y is 34 cm and 22 cm respectively, and over 70 percent of absolute value of these localization errors are less

than 12 cm. By comparison of these two experiments, it is easy to find that straight line path tracking has a better effect.

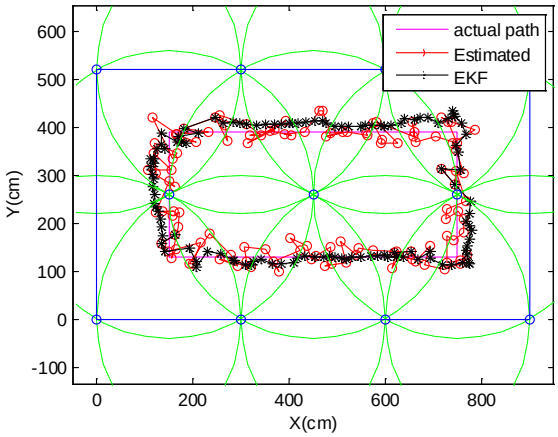

Figure 13. rectangular path tracking

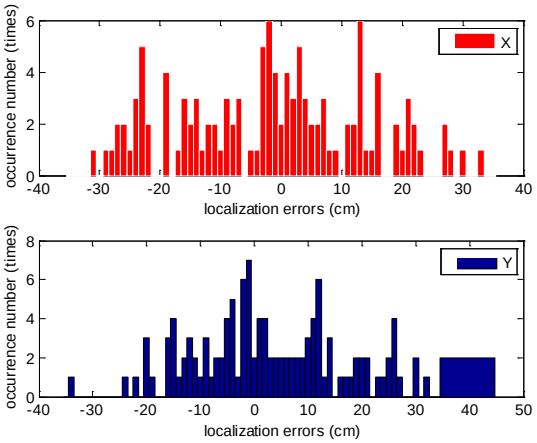

Figure 14. Histogram of localization error

The localization errors of rectangular path tracking experiments under three different velocities of smart car are listed in Table 5. Experiments show that it has the highest localization precision under $v = 100cm/s$.

Table 5: Localization errors under three different velocities

	Localization error of X direction (cm)			**Localization error of Y direction (cm)**		
	50cm/s	100cm/s	150cm/s	50cm/s	100cm/s	150cm/s
Mean	11	9	13	12	8	12
Standard deviation	8	6	9	8	5	9
Maximum	38	34	33	37	22	45

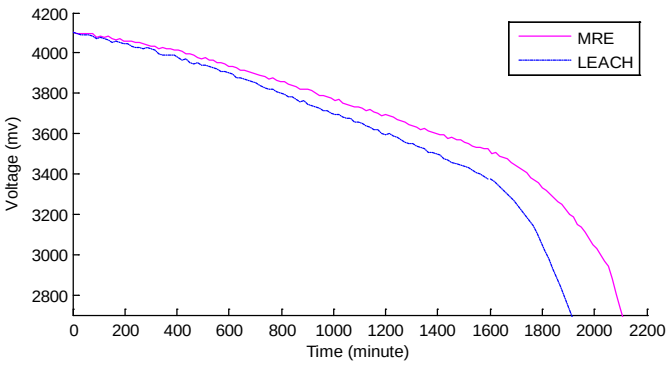

Figure 15. Endurance time of battery

Figure 15 shows the batter endurance time comparison of a cluster-head election algorithm based on maximum residual energy (MRE) and Low Energy Adaptive Clustering Hierarchy (LEACH) algorithm in rectangular path tracking experiment. A rechargeable lithium ion battery with 2500mah capacity is used in this comparative experiment, and active node sends packet at the frequency of 10 packets per second. To be convenient for comparison, all sensor nodes don't switch to sleep mode and always act as active nodes in this experiment. Each sensor node measures its battery voltage every 15 minutes. The voltage of 4200mv is regarded as maximum voltage of a rechargeable lithium ion battery, and the voltage of 2700mv is regarded as critical point of low voltage. The result shows that LEACH algorithm experiment has the endurance time of 31 hours, and MRE algorithm experiment prolongs its time over 10%, with the endurance time of 35 hours.

d. Compared with other methods

Table 6 lists the result compared with other localization methods in the quoted references

Table 6: Compared with other methods

	PILAS [10]	**PIWSNTT[11]**	**HTWDPS[12]**	**our system**
Error	50cm at actual measurement	50cm at simulation model	120cm at actual measurement	38cm at actual measurement
Advantage	Simple structure	Simple structure & wide FOV	Low computational complexity & wide FOV	Low computational complexity & minimum localization error
Disadvantage	Low efficiency	Need time synchronization; high computational complexity；	Low accuracy	

VII. CONCLUSIONS

Due to the disadvantages of traditional localization & tracking at those aspects of users' privacy protection, system configuration and maintenance, this paper presents a new method, based on radial distance modulation, to detect and locate moving object from top view angle. Our method has advantages of extracting information directly from the moving object characteristics of movement and spatial position, small computation, good robustness, convenient configuration, non-contact etc. The experiments demonstrate that although the output of PIR detectors only has two forms, "0" and "1", we can locate the moving object with simple information after modulating and encoding the perception area of sensors.

In addition, to effectively solve the problem of WSN energy imbalance, one strategy of neighbor table multicast and one electoral method of the dynamic cluster head based on the biggest energy are presented.

The localization and tracking method proposed in this paper can be widely applied in monitor system for elders living alone. The validity and feasibility of the method have been proved by the localization experiments. Since the study of the technology is still in a fledging period, these aspects of location accuracy, real-time capability and multi-object tracking, etc. need to be studied further. On the basis of preliminarily accomplished localization and tracking of moving object, what can be carried on for further studies include: human height sensing, attitude perception, typical behavior (e.g. tumbling) detection and analysis, incident recognition and so on.

ACKNOWLEDGEMENT

This paper was supported by the National Natural Science Foundation of China
(Grant no. 60775055)

REFERENCES

[1] P.Turaga, R.Chellappa, V.S.Subrahmanian and O.Udrea, “Machine recognition of human activities: A survey”, IEEE Transactions on Circuits and Systems for Video Technology, Vol. 18, No. 11, 2008, pp. 1473-1488.

[2] S.Hernandez and M.Frean, “Bayesian multiple person tracking using probability hypothesis density smoothing”, International Journal on Smart Sensing and Intelligent Systems, Vol. 4, No. 2, 2011, pp. 285-312.

[3] X.Ji and H.Liu, “Advances in view-invariant human motion analysis: A review”, IEEE Transactions on Systems, Man, and Cybernetics, Part C: Applications and Reviews, Vol. 40, No. 1, 2010, pp. 13-24.

[4] L.Wang, W.Gong, L.He, H.Xiao and Y.Huang, “Human motion recognition using pyroelectric infrared signal”, Journal of Optoelectronics. Laser, Vol. 21, No. 3, 2010, pp. 440-443.

[5] P.Wojtczuk, A.Armitage, T.D.Binnie and T.Chamberlain, “PIR sensor array for hand motion recognition”, SENSORDEVICES 2011, The Second International Conference on Sensor Device Technologies and Applications, Nice/Saint Laurent du Var, France, 2011,pp. 99-102.

[6] X.Zhao-Jun, Z.Peng-Fei and W.Bai-Kun, “Application of infrared thermal imaging in gait recognition”, Journal of Optoelectronics. Laser, Vol. 20, No. 3, 2009, pp. 402-405.

[7] R.Poppe, “A survey on vision-based human action recognition”, Image And Vision Computing, Vol. 28, No. 6, 2010, pp. 976-990.

[8] B.Song, A.T.Kamal, C.Soto, C.Ding, J.A.Farrell and A.K.Roy-Chowdhury, “Tracking and activity recognition through consensus in distributed camera networks”, IEEE Transactions on Image Processing, Vol. 19, No. 10, 2010, pp. 2564-2579.

[9] K.Morioka, S.Kovacs, J.Lee and P.Korondi, “A cooperative object tracking system with fuzzy-based adaptive camera selection”, International Journal on Smart Sensing and Intelligent Systems, Vol. 3, No. 3, 2010, pp. 338-358.

[10] G.Xue-Bin, Z.Zhi-Qiang and Y.Shi-Wei, “Research of passive infrared sensor model for wireless sensor networks”, journal of Computer Applications, Vol. 27, No. 5, 2007, pp. 1086-1089.

[11] W.Sen, C.Ying-Wen and X.Ming, “Research of Passive Infrared Wireless Sensor Network Target Tracking”, Journal of Transduction Technology, Vol. 21, No. 11, 2008, pp. 1929-1934.

[12] Q.Hao, D.J.Brady, B.D.Guenther, J.B.Burchett, M.Shankar and S.Feller, “Human Tracking With Wireless Distributed Pyroelectric Sensors”, IEEE SENSORS JOURNAL, Vol. 6, No. 6, 2006, pp. 1683-1695.

[13] J.S.Fang, Q.Hao, D.J.Brady, M.Shankar, B.D.Guenther, N.P.Pitsianis and K.Y.Hsu, “Path-dependent human identification using a pyroelectric infrared sensor and fresnel lens arrays”, Optics Express, Vol. 14, No. 2, 2006, pp. 609-624.

[14] J.S.Fang, Q.Hao, D.J.Brady, B.D.Guenther and K.Y.Hsu, “Real-time human identification using a pyroelectric infrared detector array and hidden Markov models”, Optics Express, Vol. 14, No. 15, 2006, pp. 6643-6658.

[15] J.S.Fang, Q.Hao, D.J.Brady, B.D.Guenther and K.Y.Hsu, “A pyroelectric infrared biometric system for real-time walker recognition by use of a maximum likelihood principal components estimation (MLPCE) method”, Optics Express, Vol. 15, No. 6, 2007, pp. 3271-3284.

[16] R.C.Luo, O.Chen and P.H.Lin, “Indoor robot/human localization using dynamic triangulation and wireless Pyroelectric Infrared sensor fusion approaches”, 2012 IEEE International Conference on Robotics and Automation (ICRA), 2012,pp. 1359-1364.

[17] L.Suk, N.H.Kyoung and C.L.Kyung, “A pyroelectric infrared sensor-based indoor location-aware system for the smart home”, IEEE Transactions on Consumer Electronics, Vol. 52, No. 4, 2006, pp. 1311-1317.